

Supplementary Information

Temperature-controlled, phase-transition ultrasound imaging-guided photothermal-chemotherapy triggered by NIR light

Wei Li^{#1}, Wanqing Hou^{#1}, Xiaomeng Guo¹, Lihua Luo¹, Qingpo Li¹, Chunqi Zhu¹, Jie Yang¹, Jiang Zhu², Yongzhong Du¹, Jian You^{*1}

¹College of Pharmaceutical Sciences, Zhejiang University, Yuhangtang Road 866, Hangzhou 310058, People's Republic of China

²Sir Run Run Shaw Hospital, Zhejiang University School of Medicine, Hangzhou 310016, People's Republic of China

[#] These authors contributed equally to this work

^{*} Corresponding Author:

Jian You, College of Pharmaceutical Sciences, Zhejiang University, Yuhangtang Road 866, Hangzhou 310058, People's Republic of China; Tel: 086-571-88981651; Fax: 086-571-88208439; E-mail: youjiandoc@zju.edu.cn.

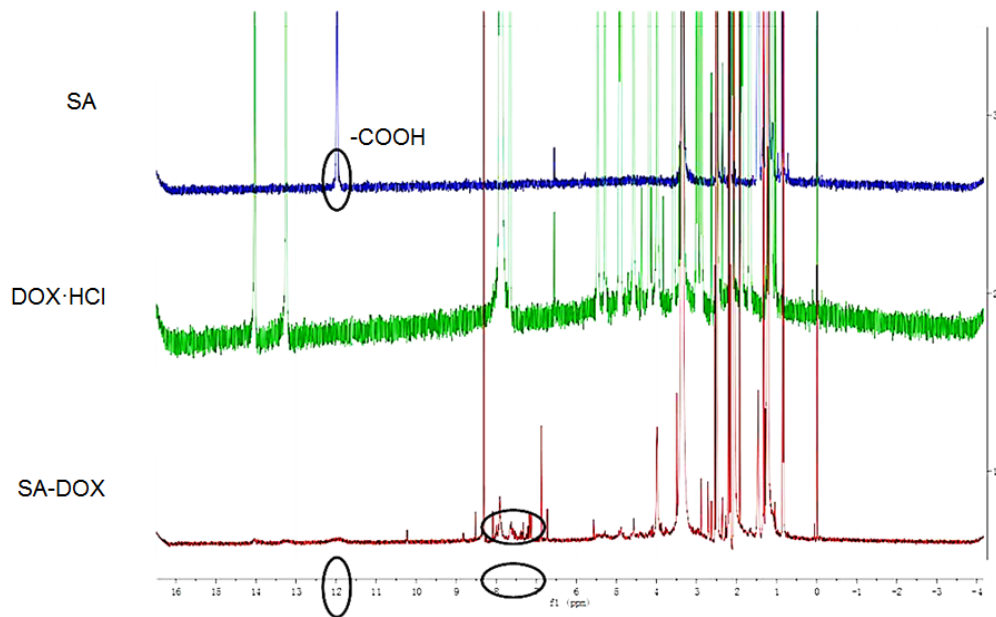


Figure S1. The $^1\text{H-NMR}$ spectra of SA, DOX·HCl and SA-DOX.

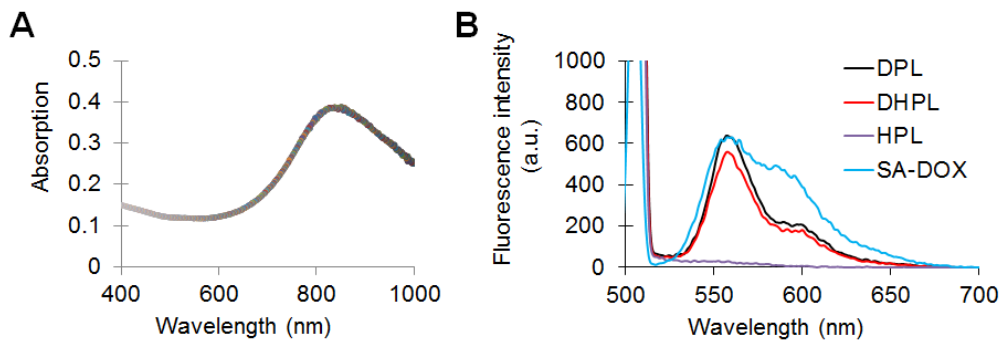


Figure S2. UV-vis and fluorescence spectra. (A) UV-vis absorption spectrum of HAuNS. (B) Fluorescence spectra of SA-DOX, DPL, HPL and DHPL (DOX/HAuNS concentration: $2.5 \mu\text{g/mL}$).

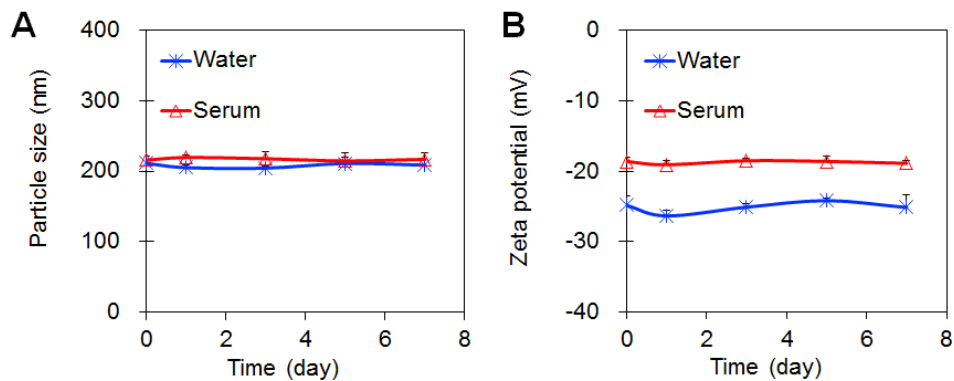


Figure S3. Stability of DHPL. (A) Particle size change of DHPL in one week (n=3). (B) Zeta potential change of DHPL in one week (n=3).

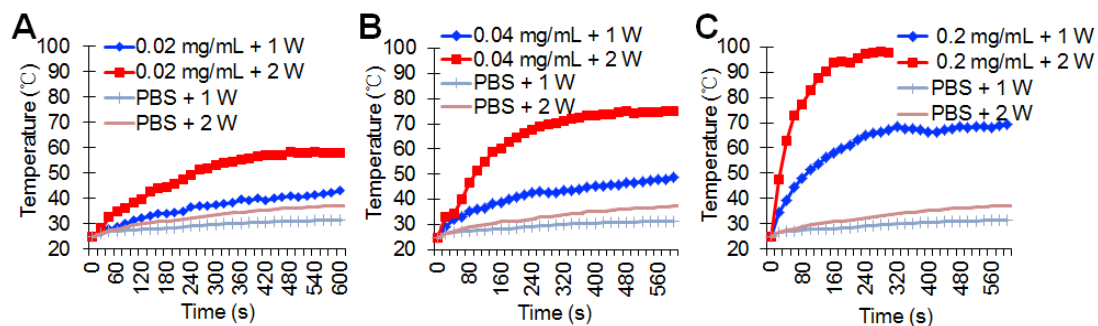


Figure S4. Photothermal effect of DHPL-59 under laser irradiation. (A) Temperature elevation curves of DHPL-59 (HAuNS: 0.02 mg/mL) or PBS under 1 W/cm² or 2 W/cm² NIR laser. (B) Temperature elevation curves of DHPL-59 (HAuNS: 0.04 mg/mL) or PBS under 1 W/cm² or 2 W/cm² NIR laser. (C) Temperature elevation curves of DHPL-59 (HAuNS: 0.2 mg/mL) or PBS under 1 W/cm² or 2 W/cm² NIR laser.

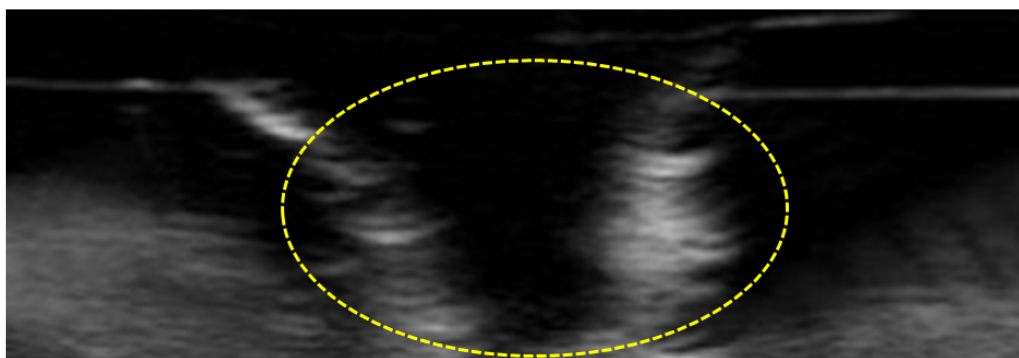


Figure S5. Ultrasound imaging of DHPL solution after “turn-off”.

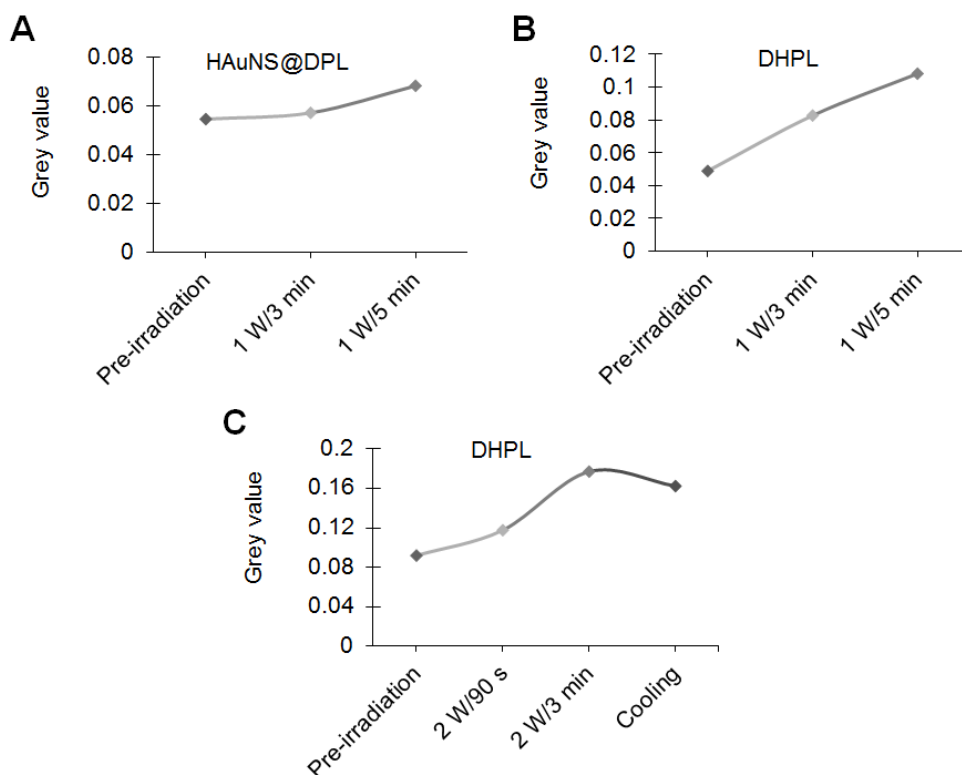


Figure S6. Gray value of the ultrasound signal of HAU@DPL (A), DHPL (B), and DHPL (cool down after laser treatment) (C) in the region of interest (ROI) under laser irradiation analyzed by “Image J” software.

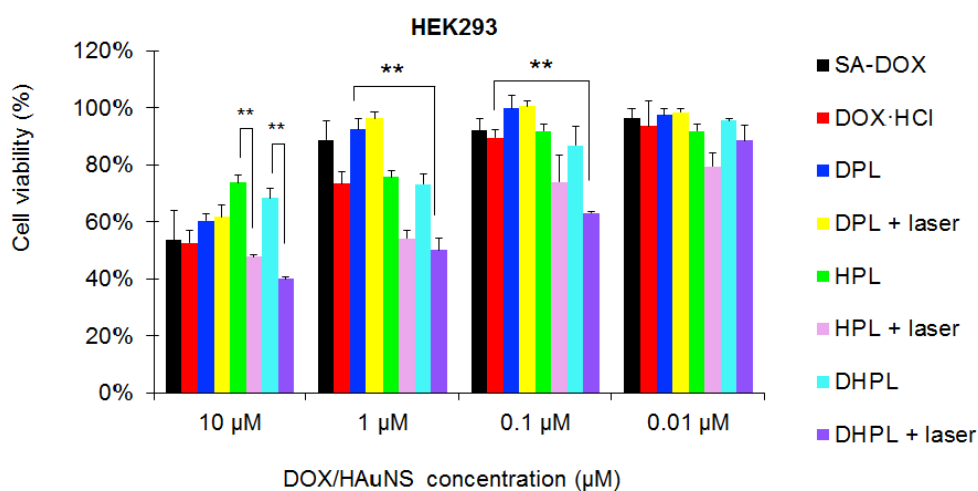


Figure S7. Cytotoxicity to HEK293 cells. Cell viability of HEK293 cells treated with SA-DOX, DOX·HCl, DPL, HPL, and DHPL followed by NIR light irradiation (1 W/cm², 3 min). Cells without laser irradiation were used as controls.

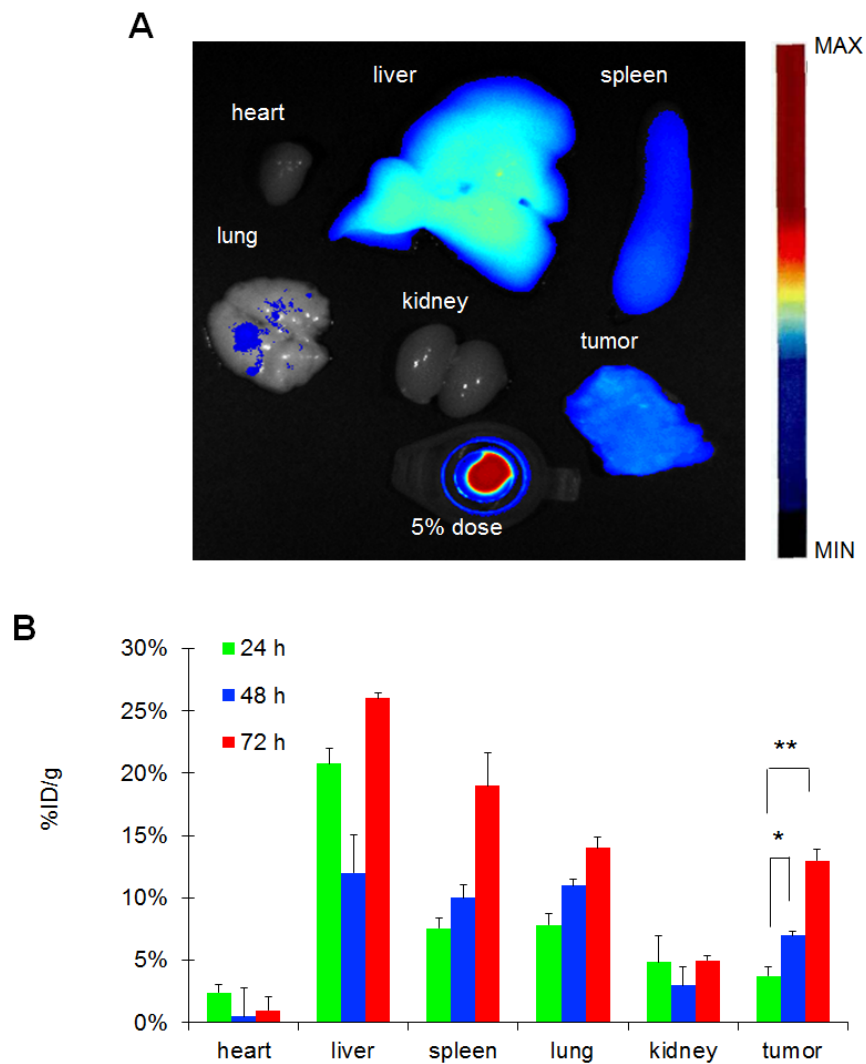


Figure S8. Biodistribution of DHPL. (A) The fluorescence imaging of various tissues at 72 h post-administration. Ex: 748 nm; Em: 780 nm. (B) Semi-quantitative fluorescence analysis of DiR-labeled DHPL in heart, liver, spleen, lung, kidney and tumor at 24, 48 or 72 h post-administration (% ID/g).

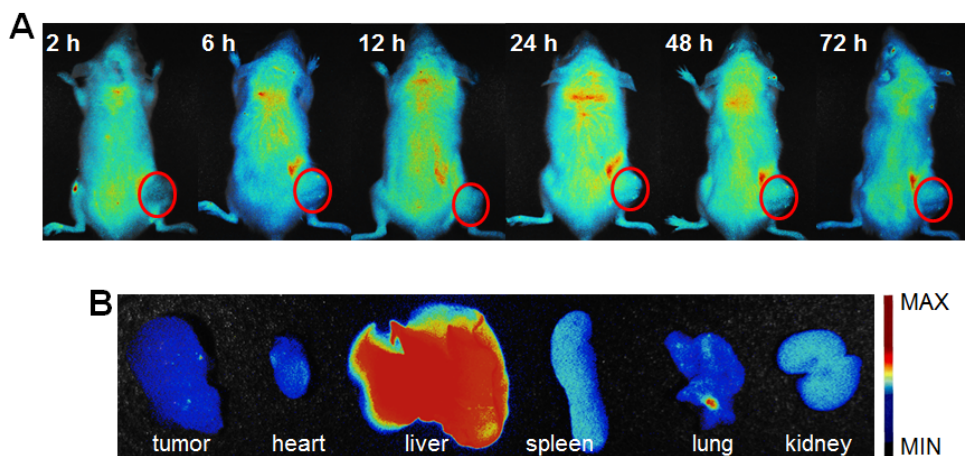


Figure S9. Biodistribution of free DiR. (A) Representative *in vivo* fluorescence imaging of the 4T1 tumor bearing mice at different time point after *i.v.* injection of free DiR. The red circles indicate tumors. Ex: 748 nm; Em: 780 nm. (B) The fluorescence imaging of various tissues at 72 h post-administration.

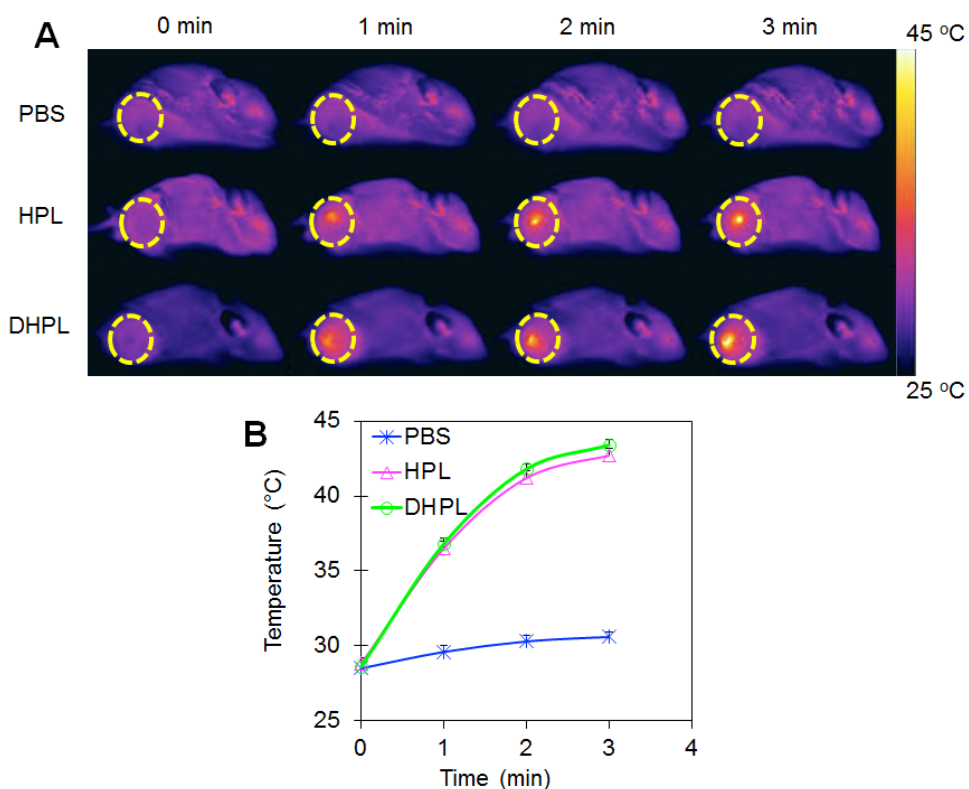


Figure S10. Thermal imaging. (A) Thermal imaging of NIR light-induced temperature elevation at tumor sites 24 h post-injection of HPL or DHPL (5 mg/kg HAuNS). (B) The corresponding temperature elevation curves in 3 min.

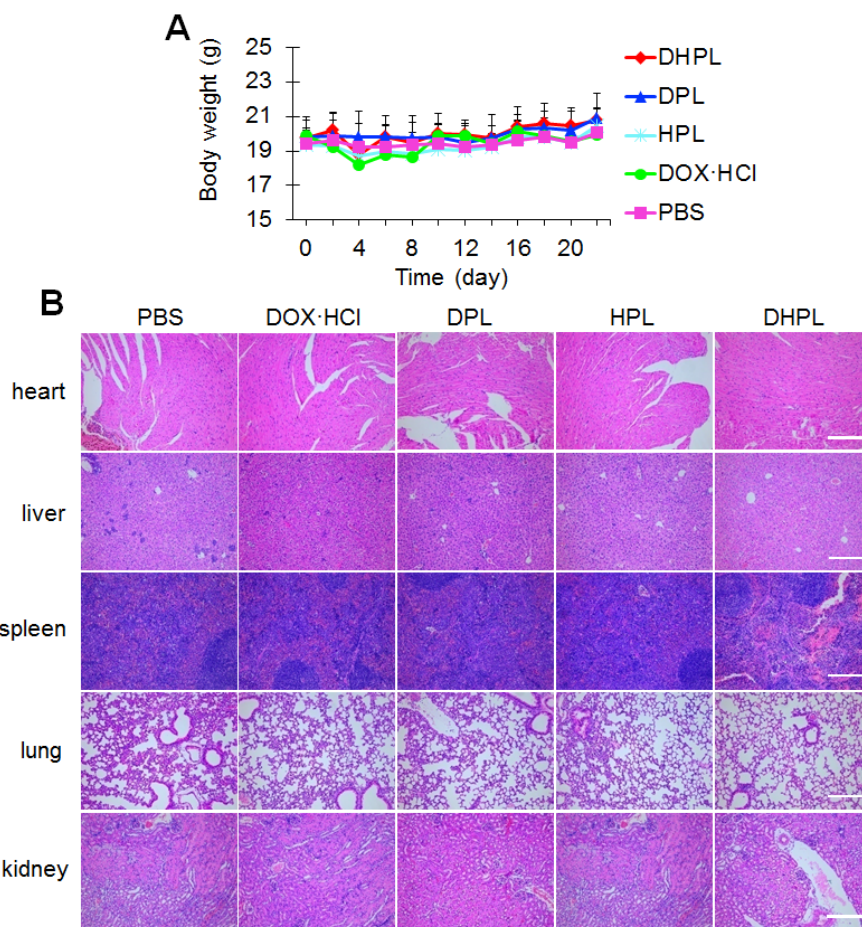


Figure S11. Safety study. (A) The body weight change curves of each group (n=7) in 22 days. **(B)** H&E-stained slices of major tissues. Scale bars, 100 μ m.